EXPERIMENTAL STUDY OF VARIABLE MASS LINER FOR SOFT X-RAY GENERATION

A.M. Bujko, V.K. Chernyshev, S.F. Garanin, Y.N. Gorbachev, V.A. Demidov,
G.G. Ivanova, V.N. Kostyukov, S.D. Kuznetsov, A.I. Kuzyaev, A.B. Mezhevov,
V.N. Mokhov, A.A. Petrukhin, V.N. Sofronov, A.I. Startsev, V.B. Yakubov

All-Russia Scientific Institute of Experimental Physics,
607200, Sarov (Arzamas-16), N.Novgorod region, Russia

Brodie G. Anderson, Carl A. Ekdahl, John L. Kammerdiener, Irvin R. Lindemuth,
Robert E. Reinovsky, Patrick J. Rodriguez, Linn R. Veeser, Stephen M. Younger,
William D. Zerwekh, David A. Poling, Ronald C. Kirkpatrick

Los-Alamos National Laboratory, New Mexico, USA

Thadeus J. Englert, Gerald F. Kiuttu

Phillips Laboratory, Albuquerque, New Mexico, USA

INTRODUCTION

High power pulsed energy sources are required to produce large amount of X-rays. The leading role in creation of ultra-high power stationary machines belongs to the US/DOE national laboratories. The machines like "Pegasus", "Saturn", "PBFA-Z" and others have been used for X-ray experiments. PBFA-Z can reach 11.4 MJ of the stored energy. Currently Atlas, storing 36 MJ is being constructed and "Jupiter" storing 120 MJ is being designed.

VNIIEF has made much progress in creation of ultra-high power explosive magnetic generators (EMG). While the hardware can be used only once, such systems allow experiments up to 200 MJ of the stored energy and up to 10^{13} W of the power in the load [1].

It is easier to perform studies of high complexity with a wide set of diagnostics on stationary machines. However, as the stored energy increases, the number of elments expended in each experiment becomes so large, that these advantages become less significant. Estimations show that the cost per shot on the stationary machine with the stored energy of ~100 MJ is higher than the experiment with EMG.

Relatively soft X-rays (quantum energy is about 0.3 keV) may be produced by acceleration of a plasma liner up to a velocity of v~300 km/s followed by stagnation in a pinch. This means that if the plasma acceleration distance is several cm, the time of plasma motion must be about 0.1 of a microsecond. This results in a difficulty, associated with the problem of plasma stability and the liner having very small thickness and very small tolerance on initial thickness and density. Besides, quick energy input into the load requires complicated fast opening switches, which need to be experimentally tested. For experiments with EMG it is reasonable to develop simpler systems to reach mass velocities about 300 km/sec. The paper [3] theoretically considers one of these systems, where a liner mass during its magnetic acceleration significantly decreases and the velocity increases, i.e., a variable mass liner (VML). The same paper suggests two experimental designs to test a new concept: full-scale experiment, including X-rays generation and a model experiment, including testing of the initial stage of VML formation (v<100 km/sec).

1. REPORT DATE **JUN 1997**	2. REPORT TYPE **N/A**	3. DATES COVERED **-**		
4. TITLE AND SUBTITLE **Experimental Study Of Variable Mass Liner For Soft X-Ray Generation**		5a. CONTRACT NUMBER		
		5b. GRANT NUMBER		
		5c. PROGRAM ELEMENT NUMBER		
6. AUTHOR(S)		5d. PROJECT NUMBER		
		5e. TASK NUMBER		
		5f. WORK UNIT NUMBER		
7. PERFORMING ORGANIZATION NAME(S) AND ADDRESS(ES) **All-Russia Scientific Institute of Experimental Physics, 607200, Sarov (Arzamas-16), N.Novgorod regio~ Russia**		8. PERFORMING ORGANIZATION REPORT NUMBER		
9. SPONSORING/MONITORING AGENCY NAME(S) AND ADDRESS(ES)		10. SPONSOR/MONITOR'S ACRONYM(S)		
		11. SPONSOR/MONITOR'S REPORT NUMBER(S)		
12. DISTRIBUTION/AVAILABILITY STATEMENT **Approved for public release, distribution unlimited**				
13. SUPPLEMENTARY NOTES **See also ADM002371. 2013 IEEE Pulsed Power Conference, Digest of Technical Papers 1976-2013, and Abstracts of the 2013 IEEE International Conference on Plasma Science. Held in San Francisco, CA on 16-21 June 2013. U.S. Government or Federal Purpose Rights License.**				
14. ABSTRACT				
15. SUBJECT TERMS				
16. SECURITY CLASSIFICATION OF:			17. LIMITATION OF ABSTRACT **SAR**	18. NUMBER OF PAGES **15**	19a. NAME OF RESPONSIBLE PERSON
a. REPORT **unclassified**	b. ABSTRACT **unclassified**	c. THIS PAGE **unclassified**			

This paper describes the first model experiment designed to test the VML concept proposed by VNIIEF to produce soft X-rays with the megajoule energy level (joint experiment "X-Ray-1" between Russia and the USA, 1995, VNIIEF).

1. EXPERIMENTAL DESIGN AND DIAGNOSTICS

Fig.1 shows the model system with VML, operating from disk EMG (DEMG) [1]. It includes three main elements:
- cylindrical liner-switch, fixed between a current conductive copper end walls;
- "clipper", providing a break in electric circuit, which causes an arc of plasma, formed between the liner and the wall;
- radial chamber, where this arc accelerates and implodes (i.e. formation of a toroidal "bubble").

A helical EMG was used to power the DEMG with the initial current. A 5-module DEMG having a diameter 40 cm was used in the "X-Ray-1" experiment.

Fig.2 schematically shows the stages in the operation of the load. In the first stage of operation, lasting tens of microseconds up to the time when DEMG reaches the current maximum, the liner-switch serves as a load. Liner was fabricated of aluminum. The initial parameters were: thickness $d=0.5$ mm, radius $r_0=196.6$ mm, mass $m=16.7$ g/cm and length $l_0=50$ mm. This experiment did not apply sophisticated methods to deliver current to the liner in a highly symmetrical way. Initial electrical contact between the liner and the wall was provided very simply: the liner was clamped between conical electrodes (the angle $\sim 12°$ relatively to the liner axis), see Fig.1. To decrease wall effects associated with the properties of strength and elasticity of liner and wall materials the liner (in a liquid state) was cut by a "clipper". As a result a current arc was formed in a portion or the with less perturbation. The minimum "clipper" radius $R_{ext}=171$ mm was chosen based on the consideration that at the clipper the liner was in a condensed state, not reaching the boiling point ($q<2$ kJ/g), in order to limit the mass of the plasma arc. The liner velocity at the clipper radius was ~ 6 km/s. The height of the clipper was 1 cm. A thick "clipper" provided attenuation of the shock wave caused by the liner impact, and consequently a higher speed and more rapid increase of the gap between the clipper and the condensed liner after the arc of plasma was formed. To provide additional attenuation of shock waves the impact area between the "clipper" and the liner was covered by a layer of foam having a density of ~ 0.5 g/cm^3. That gave us hope that unloading and spall effects at the inner surface of the clipper would be less dangerous in terms of increase of plasma arc mass.

In the second stage of operation, the liner breaks loose from the conducting wall. A high-current arc discharge appears in the gap between the liner edge and the wall. The arc of plasma, is driven through the gap by the magnetic pressure behind under the liner. This process is like the blowing up of a "bubble" of a toroidal shape, in which the material in the bubble will be only the portion in space under the condensed liner. Mass per unit area in the bubble will decrease in the process of its blowing up. Both speed and acceleration increase. Initial mass of the plasma arc is significantly less than that of the condensed liner. In the experiment, which studied the liner opening switch [5], the aluminium liner ~ 0.7 mm thick was accelerated up to a velocity of ~ 10 km/sec, the maximum current was ~ 70MA, arc mass was from 2 to 5g.

"X-Ray-1" experiment was designed in such a way that the slow condensed liner (~ 6km/s, $M_1 \sim 100$ g) could operate as a fast opening switch. The bubble, which was formed had significantly less mass ($M < 10$ g). The experiment planned to study only the initial stage of plasma shell formation and flight. Consequently the acceleration chamber was pumped to a very modest vacuum ($P_0 \sim 0.02$ mm Hg), a central measuring unit (CMU) was located at the $R_f=100$ mm. CMU surface shape was made close to the calculated shape of the bubble (Fig.1).

A wide variety of probes was located in the load: inductive, light, piezoelectric, manganine, etc. Some were located at the walls of the accelerated chamber, some were located in the CMU.

Fig.1 shows only the probes, whose signals are used in this paper to evaluate the processes in the load. The following symbols have been introduced:

•U-VNIIEF capacity voltage probe, U-PL two U-dot probes fielded by Phillips Laboratory (PL) to measure voltage derivative dU/dt, located in the transmission line at DEMG output;

•U_{res}-PL resistive probe to measure voltage at the CMU;

•ITL_i, IL_i, IWB_i-inductive current probes. ITL-probes were in the transmission line outside the liner. IL- two probes, located inside the liner at the chamber wall at the radius (R=165 mm) close to the clipper radius. Their purpose was to measure the time, when the liner breaks loose from the clipper. IWB-probes, located at the radial chamber wall (R=160 and R=122mm,) to measure the time of flight to the bubble).

•A_1-A_5, B_1-B_5, C_1-C_5 - LANL inductive B-dot probes, enclosed in three quartz tubes located outside the CMU. The probes were inserted parallel to the system axis, spaced 120° in azimuth at the R=105 mm. Each tube, 4cm long, enclosed 5 independent coils with the effective area ~6 mm^2 spaced along the tube length;

•SW_{1v}-SW_{6v} - VNIIEF light probes, located in the chamber wall (R=156 and R=107.5 mm); SW_{1v}, SW_{3v}, SW_{3v} - light collimated probes at R=156 mm

•SW_{13v}-SW_{24v} - VNIIEF light probes, located in the chamber wall (R=160 and R=122 mm);

•SK_{1v}-SK_{2v} - VNIIEF light collimated probes, located in the CMU, observing the lower part of the clipper.

•SMU_{1v}-SMU_{12v} - VNIIEF non-collimated probes located in the CMU;

•SMU_{iL} - LANL non-collimated light probes located in the CMU.

All probes in the walls at R= 160, 156, 122 and 107.5 mm were located in three equally spaced azimuthal portions.

2. ANALYSIS OF EXPERIMENTAL DATA, CHARACTERIZING OPERATION OF THE SYSTEM

Helical and disk EMG operation was checked using standard inductive probes. The DEMG was powered by a current of 7.7 MA (t=105 μsec after HEMG started its operation). The maximum current derivative was 0.21 MA/μsec. DEMG produced a current pulse with the amplitude 65 MA in the load with the maximum current derivative about 10^{13} A/sec. Fig.3 presents experimental values of the current derivative and current in the load as a function of time. Time is measured from the time of the electrical pulse firing the DEMG detonators.

The analysis of experimental data showed a deviation from the phenomena expected in the load.

First of all VNIIEF and LANL inductive probes measured that the magnetic field penetrated inside the liner very early. Fig.4 shows signals from VNIIEF inductive probe and from LANL B-dot probes. The beginning of the field penetration was observed at the 24.6-24.9 μsec (VNIIEF IL_1-IL_2 probes) and at the 24.6-28.4 μsec (LANL A_1-C_5 probes).

Second, VNIIEF light probes SMU_{iv}, located in the CMU, recorded light appearing at the joint area between the liner and the walls even during HEMG operation. Streak signals from the light probes are given in Fig.5. The earliest signals were measured by SMU_{10v} probes (φ=75°) at 2.4 μsec. The latest time for the light measured by other probes of this group SMU_{iv} corresponds to 19 μsec (SMU_{8v}, φ=315°). LANL light probes also measured early light (~23 μsec). Furthermore, LANL light probes registered impact at ~23.4 μsec apparently from plasmoids (light intensity decreased sharply, presumably as a result of plasma sticking on the light-guide surface). According to the calculations the liner breaks loose from the clipper at t=28.4 μsec (see the next section).

In this experiment we used a design (Fig.1) with "flexible" initial joint between the aluminum liner and copper conical current conductors, similar to the configuration in the paper [4]. The design turned out to be not very successful. Experimental data analysis showed that as a result of Joule heating in

the joint between the liner and the current conductor, a plasma layer under the high pressure could be formed. This layer could result in disconnecting of the elements and appearing of the resistance in the contact enough for the magnetic field and copper-aluminum plasma to penetrate inside the liner even before the liner has moved. That could be the reason for larger asymmetry in the process of bubble formation and probably for its increased mass.

Based on the measurement of collimated light probes Sk_i the following picture of the initial bubble motion was obtained. The beginning of its formation, which manifested itself by the light flash, was recorded at the time $t^{exp}_{ob}=29.3$ μsec (probe Sk_2, φ=30°). The second probe (Sk_1, φ=210°) recorded the glow $\Delta t^{exp}_{ob}=0.3$ μsec later.

The light probes at the left wall parallel to the load axis began to record the glow at the radius R=156 mm at times from 22.8 μsec (SW_{1v}-φ=90°, SW_5-φ=330°) to 25.4 μsec (SW_{3v}-φ=210°). The glow intensity increased for about 3 μsec, and within the time range 31.1 μsec (SW_{3v}-φ=210°) and 32.7 μsec (SW_{5v}-φ=330°) each of the probes measured sharp increase of the light signal, which could be associated with the bubble arriving at the radius of the probe location. Thus, angular difference in time of the bubble arrival at the radius 15.6 cm was already 1.6 μsec.

The bubble had the fastest speed at the radius R=156 mm in the angular section φ≤210°-1,5 μsec (the most intensive glow according to the probe SW_{3v} was observed at the time 32.7 μsec). Thus, the average velocity of the radial motion of the plasma shell differed azimuthally about a factor of two

Experimental data on the subsequent "bubble" expansion obtained from non-collimated light probes (from R=107.5 mm on the left wall and from R=160 and 122 mm on the right wall) does not contradict to this angular picture of the "bubble' motion and testify to further growth of its asymmetry.

We measured the voltage in the transmission line from DEMG to the load (U_{EF}, U_{PL}) by VNIIEF capacity probes and PL U-dot probes and the voltage U_0 in the CMU by PL resistive divider. A detailed analysis of those important measurements is given in the next section.

3. 1D CALCULATIONS AND PARAMETER ESTIMATIONS.OF THE DEMG LOAD AND OF THE "BUBBLE"

The main results of 1D MHD calculations for a pondermotive unit (PU) with a cylindrical liner-switch (and a transmission line (TL)) and for a variable mass liner (VML, "bubble") formed after the clipper "cuts off" a part of cylindrical liner-switch are given below.

The calculations have been made with help of a code designed to solve one-dimensional elastic-plastic and magneto-hydrodynamic problems developed on the UP program basis [5].

In these calculations the following boundary conditions for magnetic field were set on the outside $\left(R_{ext}\right)$ liner surface[1]:

$$H(t) = I_{exp}(t)/5R_{ext}(t), \qquad (1)$$

where I_{exp} is the experimental current curve in PU (see Fig.3). The magnetic field on the inside liner surfaces ($R_{int}<R_{ext}$) and the gasdynamic pressure on both liner surfaces were considered to be zero. The equation of state and the Al-liner conductivity were described by the formulas from [6]. The MHD calculations for the VML accounted for the radiant heat conduction.

---

[1] The formulas of part 2 use the system of units: $[M] = g$; $[R] = cm$; $[t] = 10^{-6} s = \mu s$;

$[I] = 10^6 A = MA$; $[H] = 10^6 Oe = MOe$; $[L] = 10^{-9} H = nH$; $[U] = 10^3 V = kV$;

$[\Phi] = 10^{-3} Wb = mWb$

According to this calculation, the liner-switch collision with the clipper started when the liner had a velocity of 3.8 km/s at t = 26.8 ms (R_{int}=17.8 cm) and was completed when the velocity was 6.0 km/s at t = 28.4 ms (R_{ext}=17.1 cm); the liner-switch collision with the CMU would have begun at t = 35.5 ms with the velocity of ~12 km/s if the liner had been accelerated by the current $I_{exp}(t)$. The U_l voltage between the initial liner contacts with the PU face walls was defined as

$$U_l = \frac{d}{dt}\left(L_l \cdot I_{exp}\right) + U_{ext},$$ (2)

where $L_l(t)$ is the inductance introduced into the current circuit by the moving liner-switch, U_{ext} is the voltage on the outside surface of this liner.

The voltage in the transmission line is

$$U_{tl}(t) = \frac{d}{dt}\left(L_{tl} \cdot I_{exp}\right) + U_{t-},$$ (3)

where $L_{tl}.$–is the inductance from the voltage measurement probes outside the liner in its initial state (~1.85nH), U_{t-} is the voltage on the TL walls resulting from the magnetic field diffusion into the walls, the $L_{tl}.$ and U_{t-} values were obtained in a similar manner as it was done for the DEMG cavities[7].

Fig.6 shows the voltages (2) and (3) and their sum $U_{cl}(t)$ which is the calculated voltage in the DEMG transmission line without the "bubble" formation account.

The "bubble" shape prior to the collision with the PU walls (see Figs.1, 2) was supposed to be a toroidal, with a toroid minor radius

$$r = R_n - R, \quad R_n \cong 17.5\ cm, \quad R<17\ cm,$$ (4)

where $R = R_{int}$ is the minimal distance of the toroid inside surface from the rotation axis, R_n is the toroid major radius which is close the clipper minimal radius. Only a small "bubble" fragment of fixed mass $M_0 = M_b / 7.5\pi$ located in the vicinity of R radius (4) was computed; here M_b is the "bubble" total initial mass. This fragment was assumed to be cylindrical and moved along the radial channel bounded by rigid walls and having the width of

$$\Delta Z = \begin{cases} 0.05cm, & R \ge 17\ cm \\ 1.75 - 0.1R, & R < 17\ cm \end{cases}$$ (5)

The 1D MHD-equations in the "channel" approximation are presented, for example, in [7]. The calculations were made from the moment $t_{ob} \cong 28.4\ ms$ which was assumed to be the start of the "bubble" formation; the initial "bubble" state in these calculations $\rho_{ob} = 2.4\ gr/cm^3$, $_{ob}= 2\ \square\square\square/\square$, $v_{ob} = 0$.

The $U_b(t)$ voltage at the formation of the "bubble" (between the clipper and the liner-switch) and the voltages $U_{b\pm}(t)$ on the inside and outside "bubble" surfaces were estimated by the formulas:

$$\left.\begin{aligned} U_b(t) &= \frac{d}{dt}\left[L_b(R,t) \cdot I_{\square\square\square}(t)\right] + U_{b-}(t), \\ U_{b-}(t) &= Z_b(R,t) \cdot E_{\square}(t), \\ U_{b+}(t) &= Z_b(R_+,t) \cdot E_{\square}(t), \\ U_{bb}(t) &= U_b(t) - U_{b+}(t). \end{aligned}\right\}$$ (6)

Here the time dependent quantities $E_-(t)$, $E_+(t)$ and $R=R_-(t)$, $R_+(t)$ are taken from the "bubble" MHD-calculations, the "bubble" inductance $L_b(R,t)$ and the efficient length $Z_b(R,t)$ of its current circuit correspond to the assumed "bubble" model and to the PU geometry (see Fig.1).

Figs. 7 - 11 represent the calculation results for M_b=7g showing "bubble" inductance $L_b(t)$, voltages (6) and the magnetic fluxes $\Phi_b(t), \Phi_{b\pm}(t), \Phi_{bb}(t)$ corresponding to them together with the $L_{bb} = \Phi_{bb} / I_{exp}$ which value is close to $L_b(t)$ value but contrary to the latter has an experimental analog $L_b(t)$.

The results given in Figs. 10–11 account the "bubble" angular time difference $\Delta t_{ef} = \pm 0.4\,ms$ which corresponds to a possible current angular asymmetry in the PU $\pm 5\%$ but is considerably less than the "bubble" experimental angular asymmetry.

For a more detailed "bubble" angular asymmetry model that took place in the experiment this asymmetry might be associated with some angular distribution of the "bubble" mass $M_b(\varphi)$ supposing that the "bubble" movement in each angular sector $\Delta\varphi$ is close to the "bubble" 1D MHD-calculation with some M_b mass. Such model does not contradict the experimental picture of the "bubble" formation and movement according to which the time difference at "bubble" formation start was considerably small ($\sim 0.3\,\mu s$), after the first 15 mm was at least 1.5 μs and increased as the "bubble" continued to move. One method of modeling of the supposed angular distribution $M_b(\varphi)$ (version M_{5b}) is given below; M_b=(6–7.5–8.5–10.5–11.5)g, $\Delta\varphi/2\pi$=(0.1–0.18–0.21–0.29–0.22) respectively.

The "bubble" parameter estimation results which are compared to the experimental data in the next part of the paper have been obtained by the "bubble" MHD-calculations described above for the M_b=7g ($\Delta t_{ef}=\pm 1.5$mcs) and for the M_{5b} version.

4. THE MAIN EXPERIMENTAL AND CALCULATION DATA DISCUSSION.

Calculationally predicted characteristics of the PU current pulse are collated in Table 1 and are compared with the corresponding experimental characteristics taken by the averaged $\bar{F}_{exp.}(t)$ curve (see Fig.3) in Table 1. The start of the "bubble" formation in the experiment t_{ob}=29.3 ms was defined from the readings of the S_{k2} collimated probe. The earlier time of 28.4 ms corresponds to the start of the opening between the liner-switch and the clipper according to MHD-calculation (see part 3); the analogous times of $t_{ob}^{(\pi)} = 28.7 \sim 30.4$ mcs were taken from the calculations before the experiment.

As it follows from the analysis of the data given in Table 1 the experiment results taking into account their errors basically agree with the preliminary DEMG+PU system results. That is clearly seen from the characteristic current values $I_0, I_{max}, I_{ob}, I_*$ which are achieved prior to the t_{ob} moment of "bubble" formation. The latter appeared close to t^*, the start of the DEMG "push". Let us note two more results.

First, the tendency $dI/dt_{exp} < dI/dt_c$ in value is evident, beginning before the moment of obtaining the dI/dt_{max} value. This can be accounted for by the additional losses of the magnetic flux in the DEMG and PU circuit, which were observed in the experiment (see part 2). Second, in the experiment a deeper minimum of current derivative $dI/dt_{min} = -9.4$ MA/ms was obtained compared to the calculations without the "bubble" formation which testifies to the actual formation of a "bubble" in the experiment.

To estimate the experimental characteristics of the "bubble" let us analyze the voltage measurement results. Fig.12 shows the $U_{PL}(t), U_{cl}(t)$ curves and correspondingly normalized $U_{EF}(t)$ curve. The characteristic behavior at $t\cong 29$ ms is less distinct on the $U_{EF}(t)$ curve. This might be partially explained by the fact that the VNIIEF probe, contrary to the PL pickup, measures the voltage averaged by azimuth. The PL measurements give the basic parameters of the non-monotonic $U_{PL}(t)$ curve mentioned: the DEMG "push" starts at $t_* = 28.7$ ms, and ends at $t = 29.4$ ms, the voltage increment in the "push" $\Delta U_* = 7$ kV. These DEMG "push" characteristics agree with analogous characteristics taken from the $U_{cl}(t)$ curve of the TL DEMG voltage. This circumstance and a good agreement of the $U_{cl}(t)$ and $U_{PL}(t)$ curves in the total time interval up to t=27 ms give grounds to reconstruct the part of the $U_{PL}(t)$ curve which is read off-scale from t=27 ms to t=28.6 ms so that at t < 29 ms the $U_{PL}(t)$ and the $U_{cl}(t)$ curves would practically coincide (at this time the "bubble" influence is not yet essential).

The difference between the experimental $U_{PL}(t)$ and the calculated $U_{cl}(t)$ voltages might be considered as the upper estimate of experimental voltage between the clipper and the liner-switch

$$U_b^{(exp)}(t) \cong U_{PL}(t) - U_{cl}(t), \quad t \geq 30 \ ms, \tag{7}$$

by means of which a certainly upper estimate of a "bubble" inductance value might be made:

$$L_b^{(exp)}(t) < \Phi_b^{(exp)}(t)/I_{exp}(t), \quad \Phi_b^{exp} = \int_{30}^{t} U_b^{(exp)}(t') dt'. \tag{8}$$

Table 1

Comparison of PU current pulse experimental values with the results of preliminary computations
(current is in MA, time in *ms*)

Current pulse characterstics	Experiment (*exp*)	Computations (*c*)
DEMG energizing current, I_0	7.5	7.5÷6.0
Current time derivative maximum, dI/dt_{max}	9.8	11.9÷10.8
Time when it is reached.	25.65	25.5÷25.4
Current maximum, I_{max}	64.4	69.6÷63.1
Time when it is reached.	27.9	28.0÷28.2
Current in the beginning of "bubble" formation, I_{ob}	63.4 ÷ 58.5	67.8÷49.8
Time when it is reached, t_{ob}	28.4 ÷ 29.3	28.7÷30.4
Current at DEMG "push", I_*	61.8	67.8÷62.3
Time of "push"beginning t_*	28.7	28.7
Time derivative of current at "push", dI/dt_{min}^*	− 6	(-4)÷(-3)
Current time derivative minimum dI/dt_{min}	-9.4	(− 7.4)÷(− 6.0)
Time when it is reached.	31.7	29.3÷29.5

Fig.13 shows the experimental $U_0(t)$ curve, its smoothed version $U^*_0(t)$ and the magnetic flux $\Phi_0(t)$ corresponding to it. This voltage assuming partial shielding by the currents recorded above the CMU might be considered as the upper estimate of the magnetic flux flowing out of the "bubble".

The upper estimate of these experimental "bubble" characteristics is due to the fact that the magnetic flux could flow through the sliding contacts between the "bubble", the liner-switch and the PU side walls. Magnetic flux might diffuse through the liner-switch as well, as the liner is distorted by the growth of its small initial pertubations.

The theoretical estimation results of the $U_{bc}(t)$ voltage at the "entrance" into the "bubble" corresponding to the $\Phi_0(t)$ magnetic flux and the "bubble" $L_{bc}(t)$ inductance are shown in Figs. 14,15 compared to the estimations by the experimental $U_{PL}(t)$ and $U_{EF}(t)$ curves. The estimated results of the

$U_{b+}(t)$ voltage on the "bubble" outside surface and the corresponding magnetic flux $\Phi_{b+}(t)$ are shown in Fig.16 compared to the experimental $U_0(t)$ and $\Phi_0(t)$ values. Fig.17 gives the comparison of experimental voltages in PU DEMG with analogous calculated voltage

$$U_c(t) = U_{cl}(t) + U_{bc}(t), \tag{9}$$

where $U_{bc}(t)$ is the voltage at the "entrance" of the "bubble". These comparisons use the results of the "bubble" MHD-calculation with the M_b=7g mass.

The analogous comparison of the theoretical estimate of the "bubble" characteristics for the M_{5b} version with corresponding experimental data is shown in Figs.18-20.

It is evident from the results given in Figs.14-20 that the experimental and calculated data are generally in satisfactory agreement, taking account of their considerable errors. Let us note that the fine structure in the main peak of the experimental curve $U^*_0(t = 32 \sim 38~\mu s)$ is qualitatively and in some parameters quantitatively depicted better in the M_{5b} version than in the case with M_b=7 g calculation. In particular, two late peaks at t = 36 ~ 38 ms are reproduced by the contribution of M_b=10.5 g and 11.5 g values and the calculated $\Phi_{b+}(t)$ and experimental $\Phi_0(t)$ magnetic fluxes agree better.

The observed picture of the "bubble" movement (see part 2) might be explained in the following way in the frames of the "bubble" $M_b(\varphi)$ model.

The fastest "bubble" movement takes place in the angular sector $\varphi \approx 210°$, corresponds to the "bubble" smallest sector mass $M_b^{(min)} \approx 5.5~g$, here the "bubble" maximum velocity was obtained. The value of this sector is ~10%. The "bubble" collision with the CMU in this angular sector defines the first peak ($t \approx 33~\mu s$) in the fine structure of the experimental voltage $U^*_0(t)$ recorded at CMU. The calculated time of the arrival of the "bubble" hot part at the 15.6 cm radius corresponds approximately to the experimental start of maximum glow recorded by the CW...photo collimated probe $S_{W3}(\approx 31.2~\mu s)$.

The slowest "bubble" movement took place in the angular sector $\varphi \approx 330°$ and corresponds to the $M_b^{(max)} \approx 11~g$ maximum sector mass. Here the "bubble" maximum velocity is ~20 km/s, the sector dimension is 15-20%. This "bubble" mass collision with the CMU defines the latest peak ($t \approx 37~\mu s$) in a fine structure of $U^*_0(t)$ voltage experimental curve. The calculated time of arrival of the "bubble" hot part in this angular sector to the S_{W5} collimated light probe placed on the 15.6 cm radius corresponds approximately to the experimental ($\approx 32.7~\mu s$).

In the intermediate angular sectors whose total sum is 70-75% the "bubble" was characterized by the "leading" sector masses M_b close to 10 g, 9 g, 8 g and 7 g. The latter of these sector masses has defined the central peak ($t \leq 34~\mu s$) in a thin structure of the $U^*_0(t)$ experimental curve main peak. The calculated time when the "bubble" reaches S_{W1} collimated light probe placed in the angular sector $\varphi \approx 90°$ on the 15.6 radius in this sector corresponds approximately to the experimental moment $\approx 31.7~\mu s$. when the "bubble" hot part appeared here. The calculated profiles of the MHD-values in the "bubble" at this moment are shown in Fig.8 (density ρ, velocity v, magnetic and electric fields H and E, temperature T). The velocity of the "bubble" impact on the CMU in this sector is more than 30 km/s.

The picture of the "bubble" possible angular asymmetry built by these three angular sectors (φ=90°,210°,330°) is presented in Fig.21; here the maximal angular asymmetry of the "bubble" before its impact on the CMU reaches $(\varnothing_b-\varnothing_{CMU})/\varnothing_{CMU}\cong0.17$.

CONCLUSION

The pulse power system with the liner load (helical EMG, disc EMG, the transmission line and aluminum liner before the plasma "bubble" formation have functioned in the experiment, in a whole, according to preliminary calculations. In particular, the values of maximum current ~65 MA and the current at the time of the supposed "bubble" formation start ~.64 MA obtained in the experiment are within the range calculated before the experiment for these parameters: 70 ÷ 63 MA and 68 ÷ 50 MA respectively.

Valuable information on the liner PU operation including the process of the plasma "bubble" formation has been obtained. The results of theoretical and computational analysis of the experimental data definitely indicate the formation of a plasma "bubble", a main new phenomenon expected in the experiment. The "bubble" basic experimental parameters have been estimated: a total mass ~7 g, maximum velocity at the collision with the CMU~50 km/s, angular asymmetry, etc. Besides this, the experiment has shown the presence of considerable discrepancies in the experimental behavior of the liner PU unit compared to the expected one. These discrepancies, first of all, comprise an unexpectedly large angular asymmetry in the processes accompanying the plasma "bubble" formation, a very early appearance of the currents and, possibly, plasma in the central area under the liner and a large "bubble" mass as well. A possible reason for deviation from the expected phenomenon and of the differences mentioned might be an insufficiently uniform contact of aluminum liner with copper conical current-feeders. We suppose that the area of the insufficiently good contact caused overheating by joule heat and might be the cause of unexpected copper-aluminum plasma and magnetic field penetration inside the liner and might be the cause of a large asymmetry and, probably, higher "bubble" masses. We hope to change the liner unit design so that to provide a reliable liner contact with the walls and to avoid the side effects described above and to diminish the initial mass of the plasma "bubble".

REFERENCES

1. V.K. Chernyshev, M.S. Protasov, V.A. Shevtsov, A.A. Petrukhin, V.B. Yakubov, et al., "Explosive magnetic generators of "Potok" family", Eighth IEEE Intern. Pulsed Power Conference, San-Diego, 1991.

2. P.J. Turchi, J.F. Davis, M.L. Alme, G. Berd, C.N. Boyer, S.K. Coffey, D. Conte, S.W. Seiler, W.L. Baker, J.H. Degnan, D.J. Hall, J.L. Holmes, W.F. McCullough, D.W. Price, M.H. Frese, R.E. Peterkin, N.F. Roderick, J.D. Graham and E.A. Lopez, "Generation of High-Energy x-Radiation Using a Plasma Flow Switch. J. Appl.

3. A. M. Buyko, O. M. Burenkov, V. K. Chernyshev, S. F. Garanin, S. D. Kuznetsov, A. I. Kuzyayev, V. N. Mokhov, I. V. Morozov E. S. Pavlovsky, À. À. Petrukhin, A. I. Startsev, V. B. Yakubov, B. G. Anderson, C. A. Ekdahl, J. Kammerdiner, I. R. Lindemuth, R. E. Reinovsky, P. Rodriguez, P. J. Sheehey, L. R. Veeser, S. M. Younger, B. Zerwekh "CHANGING MASS LINER SYSTEM FOR GENERATION OF SOFT X–RADIATION", Zababahin Science Readings, Chelyabinsk-70, 1995

4. À. À. Petrukhin, N. P. Bidylo, S. F. Garanin, V. M. Danov, V. V. Zmushko, A. I. Kuzyayev, V. N. Îîkhîv, E. S. Pavlovsky, À. À. Prokopov, M. S. Protasov, V. K. Chernyshev, V. A. Shevtsov, V. B. Yakubov. "Current pulse generation using an opening switch actuated by magnetic field." //Ultrahigh magnetic fields. Physics. Technology. Application. /Ed. by V. M. Titov, G. A. Shevtsov. Moscow, Nauka Publishers, 1984. p. 406.

5. V. A. Batalov, V. A. Svidinsky, V. I Selin, V. N. Sofronov "UP code for solution of one dimensional gasdynamic and plastic–elastic problems of continuous media mechanics", VANT Methods and programs of numerical solution of mathematical physics problem, 1978, 1(1), p.21

6. A. M. Buyko, S. V. Garanin, V. A. Demidov et al. "Investigation of the dynamics of a cylindrical exploding liner accelerated by a magnetic field in the megagauss range". Megagauss fields and pulsed power systems (MG-V). 1989,p.743.

7. A. M. Buyko, V. M. Danov, V. I. Mamyshev, V. B. Yakubov. A technique for numerical simulation of disk exploded magnetic generator with electro – exploded current opening switch and liner load (VANT, Mathematical modeling of physic processes, 1995,4,p.12) .
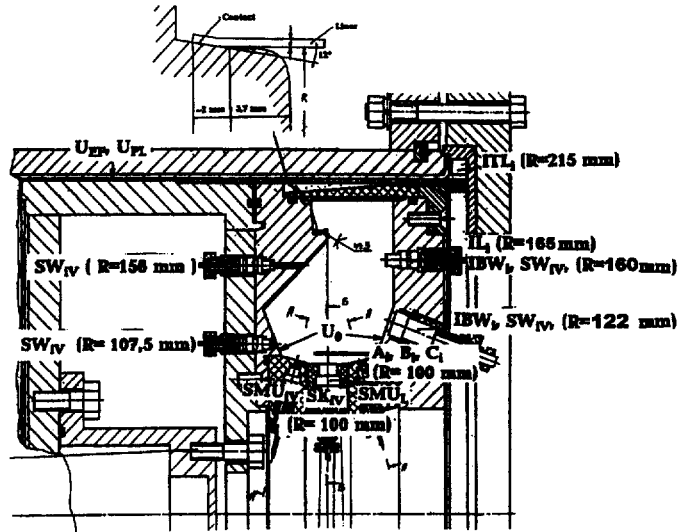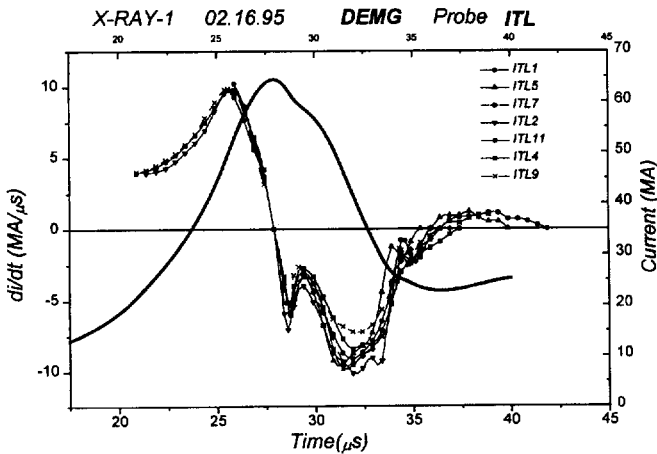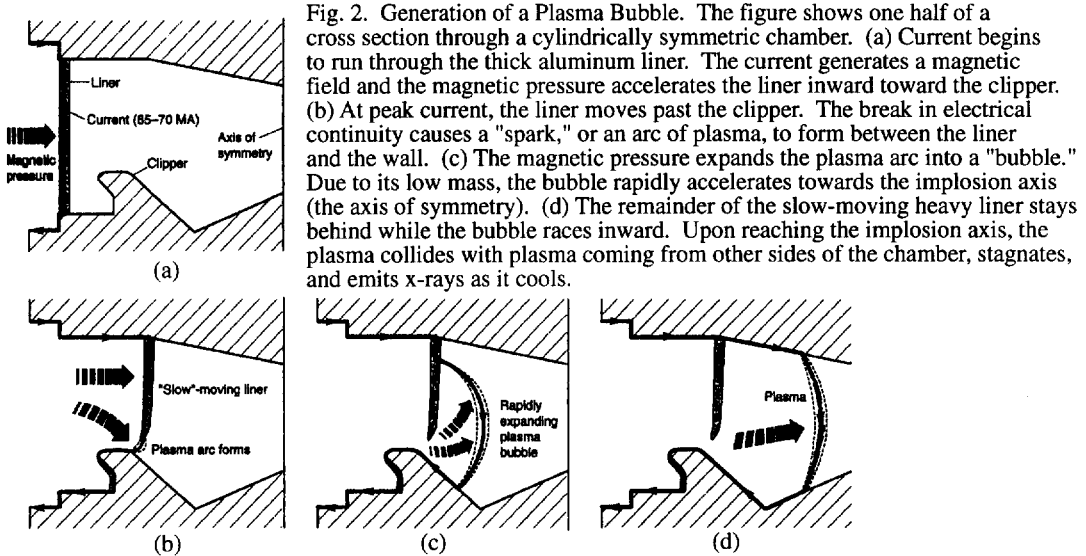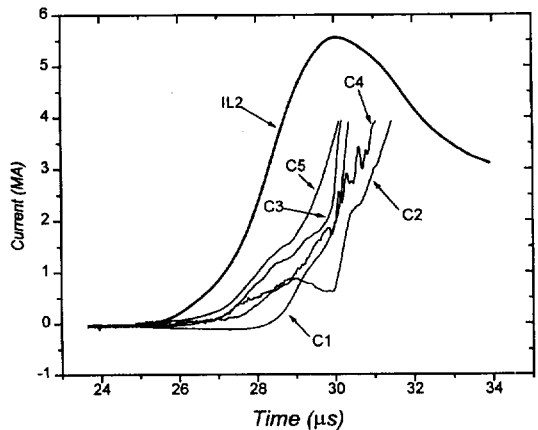
Fig. 1

(a)

Fig. 2. Generation of a Plasma Bubble. The figure shows one half of a cross section through a cylindrically symmetric chamber. (a) Current begins to run through the thick aluminum liner. The current generates a magnetic field and the magnetic pressure accelerates the liner inward toward the clipper. (b) At peak current, the liner moves past the clipper. The break in electrical continuity causes a "spark," or an arc of plasma, to form between the liner and the wall. (c) The magnetic pressure expands the plasma arc into a "bubble." Due to its low mass, the bubble rapidly accelerates towards the implosion axis (the axis of symmetry). (d) The remainder of the slow-moving heavy liner stays behind while the bubble races inward. Upon reaching the implosion axis, the plasma collides with plasma coming from other sides of the chamber, stagnates, and emits x-rays as it cools.

(b)   (c)   (d)

Fig. 3

Fig. 4

Fig. 5. Light signals from the optical pins.
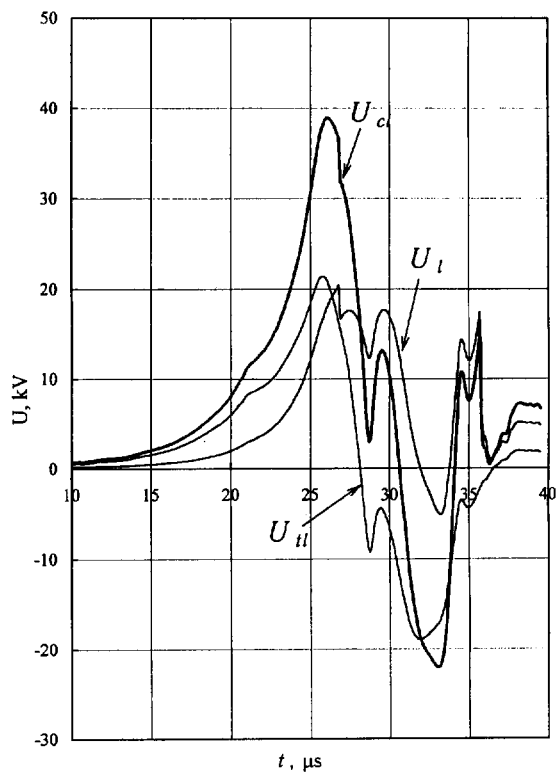
Fig. 6. Computational load voltage without accounting for "bubble" formation U_{cl} and its components (2) and (3).
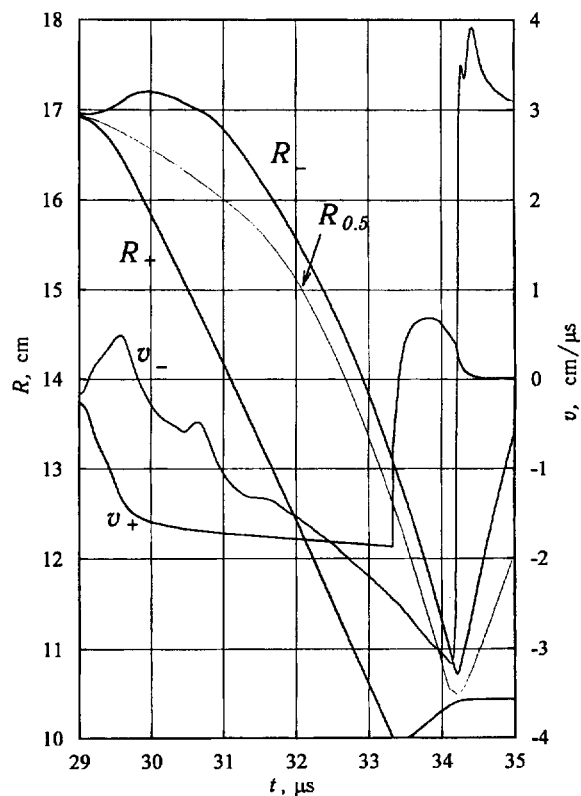
Fig. 7. The (R-t) and (v-t) diagrams of movement of the "bubble" surfaces from computation with $M_b = 7$ g.
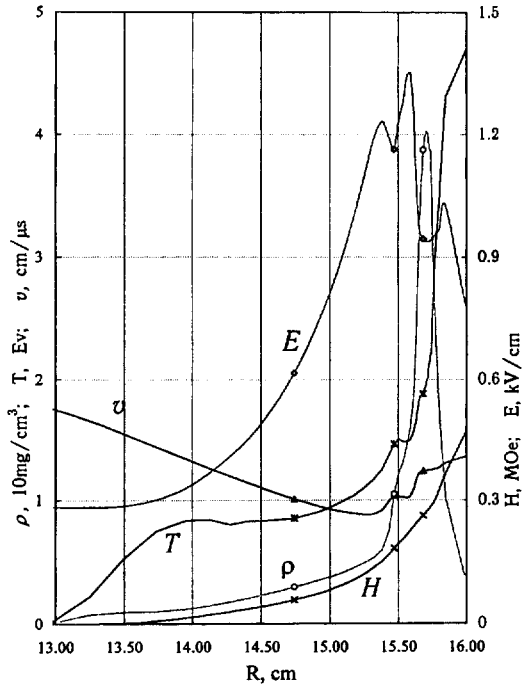
Fig. 8. Profiles of MHD-values th "bubble" approaching the collimated light probes CW_{1V}, CW_{3V}, and CW_{5V} ($M_b = 7$ g).
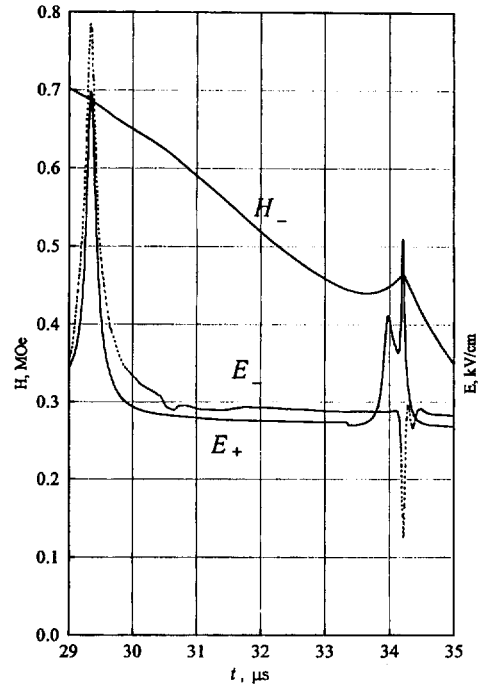
Fig. 9. Magnetic H and electric E field intensities on the external (+) and internal (-) "bubble" surfaces ($R_+ < R_-$) from computation with $M_b = 7$ g.
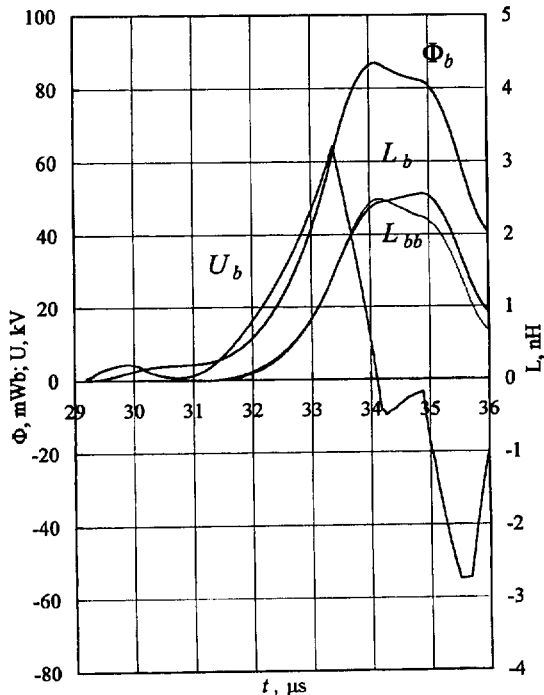
Fig. 10. Voltage U_b between the cutoff and the condensed liner and the corresponding magnetic flux Φ_b, inductances L_b and L_{bb} of the "bubble" from computation with $M_b = 7$ g ($\Delta t_{ef} = 0.8$ μs).
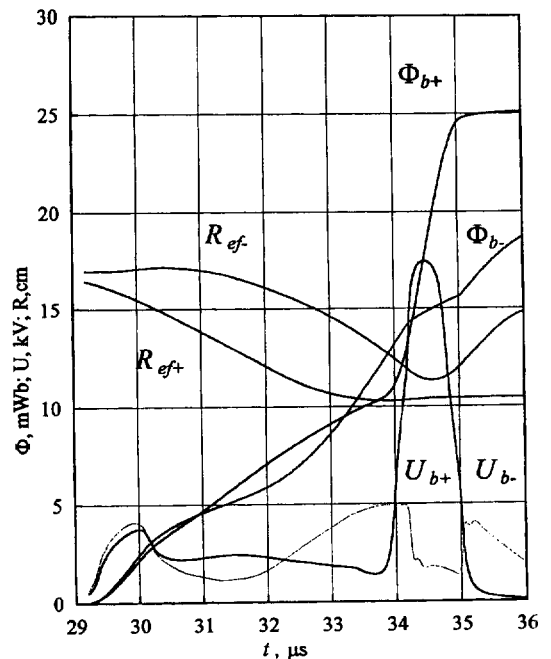
Fig. 11. Voltages $U_{b\pm}$ (2.7) and the corresponding magnetic fluxes $\Phi_{b\pm}$, the effective radii $R_{ef\pm}$ of the external (+) and internal (-) "bubble" surfaces from computation with $M_b = 7$ g ($\Delta t_{ef} = 0.8$ μs).
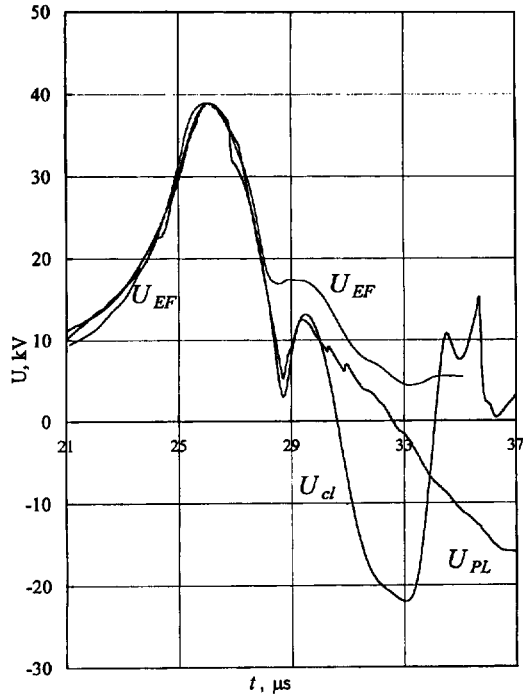
Fig. 12. Comparison of experimental voltage in the DEMG TL (U_{PL}, U_{EF}) with computational voltage U_{cl} obtained without accounting for "bubble" formation.
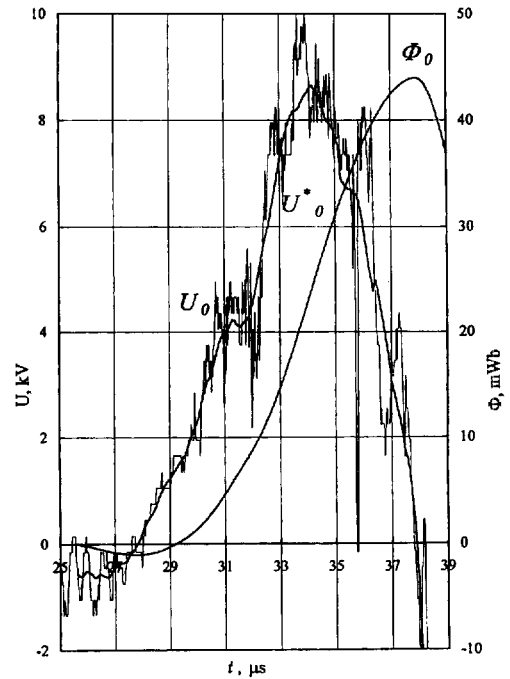
Fig. 13. Experimental voltage U_0 on the CMU and the corresponding magnetic flux Φ_0(U^*_0 — the smoothed curve of U_0.
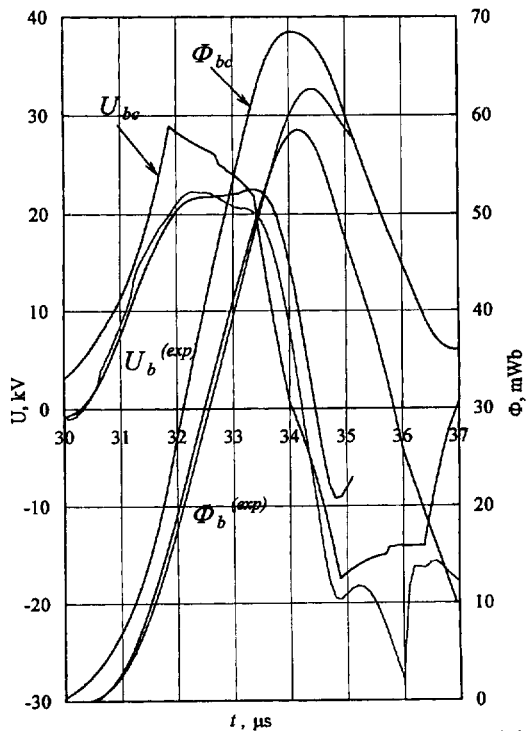
Fig. 14. Comparison of evaluations of experimental and computational voltages between the clipper and the liner and of the corresponding magnetic fluxes (for $M_b = 7$ g).
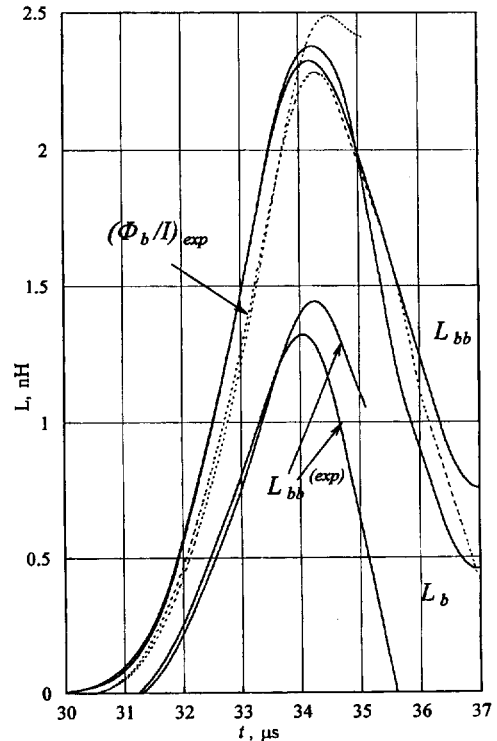
Fig. 15. Comparison of evaluations of experimental and computational "bubble" inductances (for $M_b = 7$ g).
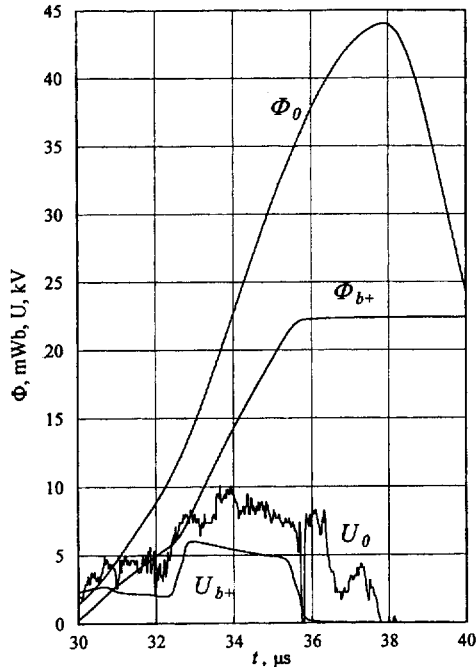
Fig. 16. Comparison of experimental voltage U_0 with voltage on the external "bubble" surface U_{b+} from computation with $M_b = 7$ g ($\Delta t_{ef} = \pm 1.5$ μs) and comparison of the corresponding magnetic fluxes.
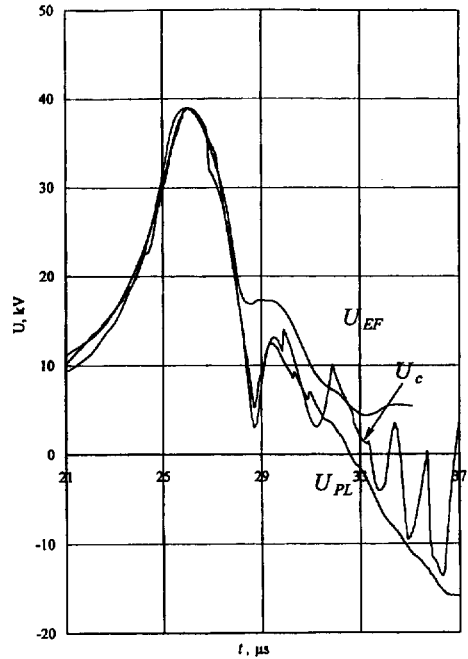

Fig. 17. Experimental U_{PL}, U_{EF} and computational U_c voltages in the DEMG TL (from computation with $M_b = 7$ g).
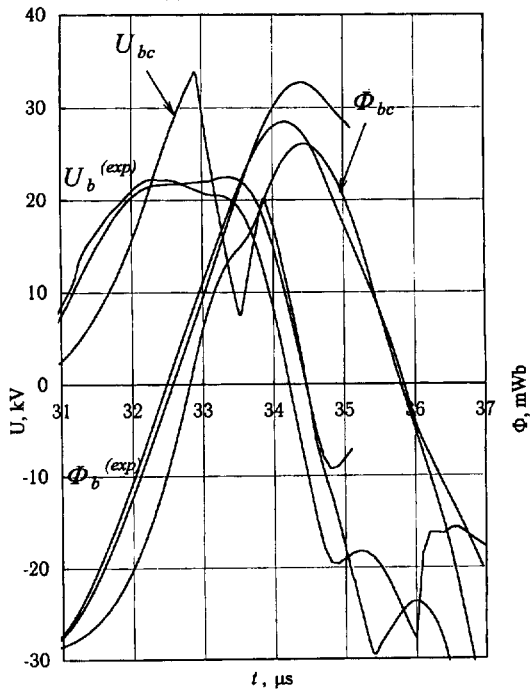

Fig. 18. Comparison of evaluation results of experimental and computational voltages between the cutoff and the condensed liner and of the corresponding magnetic fluxes (case M_{5b} (ϕ)).
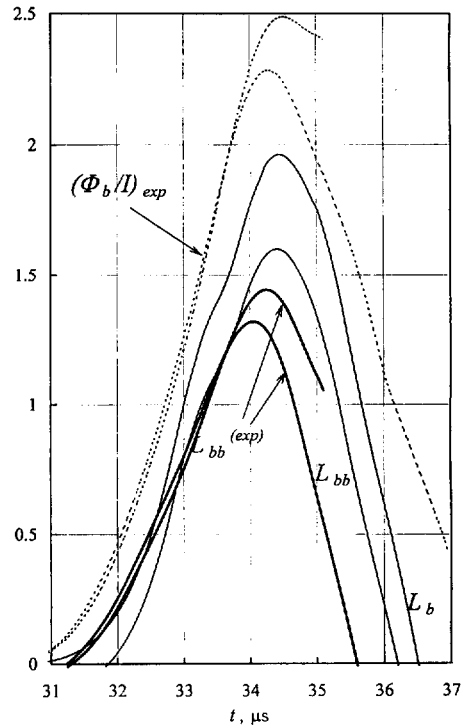

Fig. 19. Comparison of evaluation results of experimental and computational "bubble" inductances (case $M_{5b}(\phi)$).
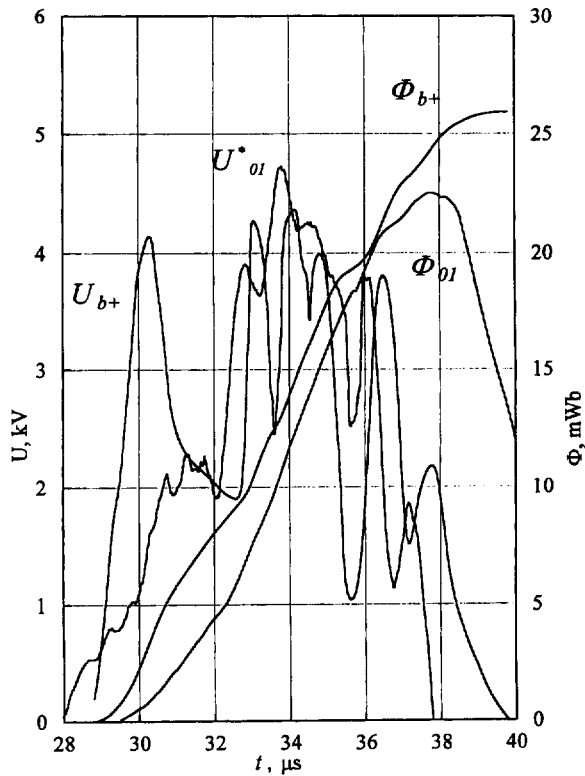
190

Fig. 20. Comparison of experimental voltage U^*_{01} with voltage on the external "bubble" surface U_{b+} for $M_{5b}(\phi)$ case and comparison of the corresponding magnetic fluxes.
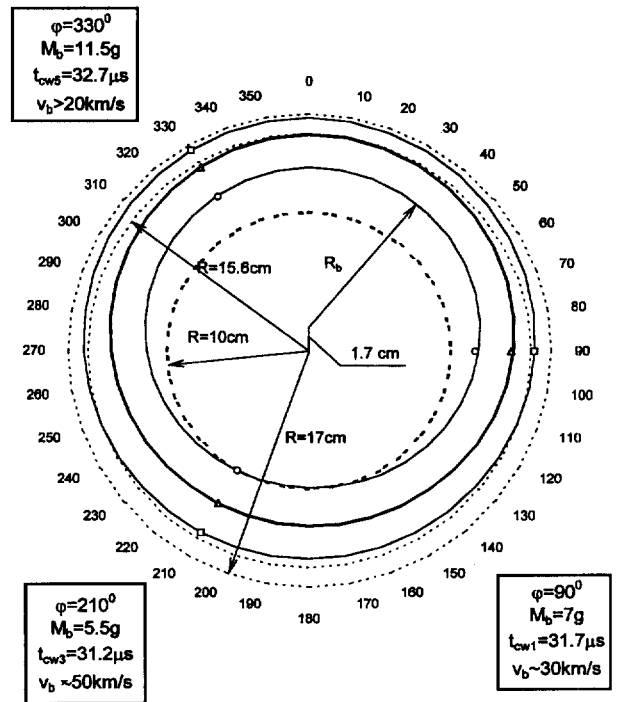
Fig. 21. Possible angular asymmetry of the "bubble" prior impact on the CMU ($t < 32.4\ \mu s$).